Non-Uniform Markov Random Fields for Unsupervised Classification of SAR Images

Sylvain Lobry, LTCI, CNRS, Télécom ParisTech, Université Paris-Saclay, sylvain.lobry@telecom-paristech.fr, France
Florence Tupin, LTCI, CNRS, Télécom ParisTech, Université Paris-Saclay, florence.tupin@telecom-paristech.fr, France
Roger Fjørtoft, CNES, roger.fjortoft@cnes.fr, France

Abstract

When dealing with SAR image classification, class parameters may vary along the swath due ti the antenna pattern. When this pattern is not corrected, traditional classification algorithms are not adapted as they assume constant class parameters across the image. In this paper, we propose a binary classification algorithm based on Markov Random Fields that into account the parameters variations along the swath.

1 Introduction

Because of its robustness to weather changes, SAR acquisition is often used for mapping or change detection. These methods often rely on a classification step making it one of the primary challenges of SAR image processing.

In this paper, we propose a binary classification method adapted to parameters variations of the classes along the swath. This phenomenon may appear when the antenna pattern is not fully corrected, which can be the case on airborne SAR and occasionally for spaceborne SAR. One reason for not applying this correction is when a class presents a weak signal; correcting the pattern would result in varying parameters for such a class in the image, which is, among others, the case for SWOT mission [5]. SWOT principal instrument (named KaRIn) operates in the Ka band (35.6GHz) in near nadir. In images acquired with such an instrument, non-water elements have a low backscattering, preventing from using a pattern correction step. In this paper, we presents an approach taking into account the variations inside a class to allow classification on such images.

In section 2, the proposed model is introduced. An exact optimization method of this model is presented in section 2.3. Finally, we present the results on TropiSAR and SWOT data in section 3.

2 Non-Uniform Markov Random Fields

Given a set of sites $\mathcal{S} = \{s_i, 0 \leq i < N_s\}$, we consider two random process:

- $\mathbf{V} = (V_s)_{s \in \mathcal{S}}$ which models the observed image to be classified;

- $\mathbf{U} = (U_s)_{s \in \mathcal{S}}$ which models the result of the classification.

In the previous definitions, $V_s \in \mathbb{R}$ and each site of $\mathbf{U}$ have the value of its corresponding label; $U_s \in \Lambda = \{\lambda_i, 0 \leq i < N_\lambda\}$. In the rest of this article, we only consider the case of binary classification (i.e. $N_\lambda = 2$) even though the proposed method could be adapted to multi-label problems.

Realizations of $\mathbf{V}$ and $\mathbf{U}$ are named $\mathbf{v} = (v_s)_{s \in \mathcal{S}}$ and $\mathbf{u} = (u_s)_{s \in \mathcal{S}}$ respectively.

Our goal is to find the realization $\hat{\mathbf{u}}$ of $\mathbf{U}$ that best explains the observation $\mathbf{v}$. Following the work of [6], this can be expressed as:

$$\hat{\mathbf{u}} = \arg \min_{\mathbf{u}} - \log\left(\mathrm{p}(\mathbf{v}|\mathbf{u})\right) - \log\left(\mathrm{p}(\mathbf{u})\right)$$
$$= \arg \min_{\mathbf{u}} \mathcal{E}(\mathbf{u}), \qquad (1)$$

involving the likelihood $\mathrm{p}(\mathbf{v}|\mathbf{u})$ of the observation considering the chosen classification and a prior on the classification result $\mathrm{p}(\mathbf{u})$.

2.1 Prior definition

On such classification tasks, a widely-used prior is to enforce spatial coherence for the classes between neighbor pixels. When using only 2 labels, a common prior is Ising model:

$$- \log\left(\mathrm{p}(\mathbf{u})\right) = \sum_{s,t \in \mathcal{C}} \beta |u_s - u_t|, \qquad (2)$$

where $\mathcal{C}$ is the set of all cliques in $\mathcal{S}$ depending on the chosen neighborhood (4 or 8 connexity).

2.2 Likelihood definition

In the case of intensity SAR images, noise follows a Gamma distribution ([7]) and can be considered separable:

$$\mathrm{p}(\mathbf{V} = \mathbf{v}|\mathbf{U} = \mathbf{u}) = \prod_{s \in \mathcal{S}} \mathrm{p}(V_s = v_s|U_s = u_s), \quad (3)$$

The likelihood $p(V_s = v_s | U_s = u_s)$ is usually chosen for each class i:

$$p(V_s = v_s | U_s = i) = \frac{1}{\Gamma(L)} \frac{L}{\mu_i} \left(\frac{L v_s}{\mu_i} \right)^{L-1} e^{-\frac{L v_s}{\mu_i}},$$
(4)

where L is the number of looks of the image and μ_i is the mean of the class i which can be estimated, given a previous classification $\mathbf{u}_{prev}$, by the maximum-likelihood estimator:

$$\hat{\mu_i} = \frac{1}{|\mathcal{S}_i|} \sum_{s \in \mathcal{S}_i} v_s,$$
(5)

where $\mathcal{S}_i = \{s, u_{prev,s} = i\}$. When the pattern correction step has not been performed or classes have an important intra-class variation, using only one parameter for each class does not yield good results. We show the variation of the true mean parameter for water and background classes in a simulated SWOT SAR image in **Figure 1**. The red curve shows the mean parameter when computed on the whole image. When compared to the blue curve, we can see that the mean computed on the whole image is neither representative of the extremities nor the center of the image.
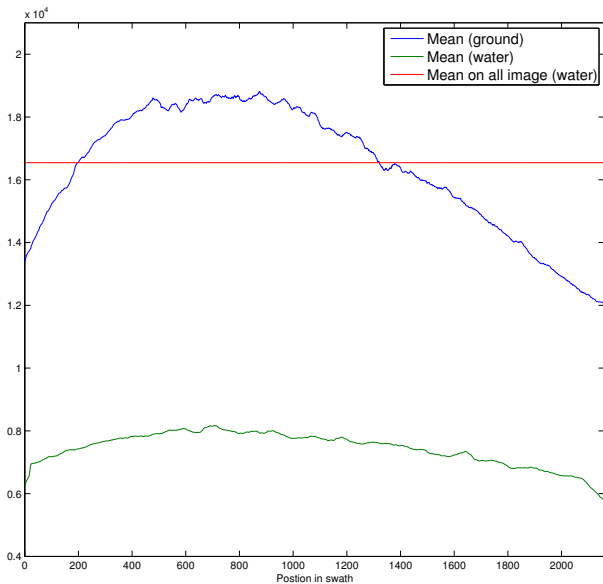
Figure 1: Parameters of SWOT image depending on the position in the swath. Input image provided by [4].

To take into account the variations in the image, we propose to use several parameters for each classes by partitioning the image in region on which to compute the parameters.

Image partitioning We seek a partitioning of the image so that each region fills the following requirements:

- Each region of the partition should be small enough so there is almost no variation of the parameters in it ($\mathcal{R}_1$);

- it contains enough pixels of the two classes so that the maximum likelihood estimator is good enough ($\mathcal{R}_2$).

To obtain such a partition, we propose to use quadtrees ([9]). Quadtrees have been extensively used in image coding ([10]) and in segmentation ([1]).
The partitioning process follows:

1. Starting from a region (for the first iteration, the region is the whole image) and a classification (obtained either using a previous classification, KMeans or a threshold for the first iteration, and a previous classification for the next ones), we try to find a partitioning in 4 regions of equal size fulfilling the 3 requirements.

2. If at least one of the regions breaks one of the requirements, we try to realize a partition containing 2 regions, first by doing a vertical cut, then an horizontal cut.

3. If a partition has been performed in the previous 2 steps, the newly created regions are partitioned again starting from step 1 after the parameters have been estimated and a new classification has been performed. If no partition was found, we stop for this region and try another one.

4. We stop the process when no region can be divided.

In practice, the requirements on small regions is obtained by dividing the regions and never prevent a division. The second requirement (each class must be represented) is verified by checking that the least represented class is over a given percentage (in the following: 10%). Finally, a parameter tuning the minimum number of elements in the region is used for the third requirement (in the following: 2500 points).

Preventing the apparition of a degenerate case When we check that every classes are present in the regions, it is done using a previous classification that is imperfect. Thus, if the classification used is too bad, we could be in a case where we try to realize a binary classification when there is only one class in the region. To limit the influence of the initialization case, a regularization step enforcing smooth variations along the swath is done.
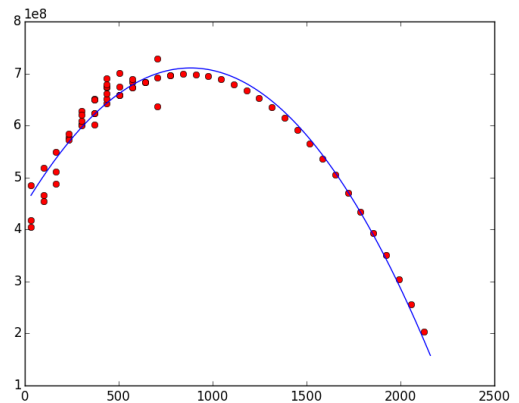
Figure 2: Regularization curve for the parameters of water class in **Figure 4**

At each iteration, a Least-Squares Fitting of a second order polynomial on the values of the parameters of the regions is performed with respect to the position in the swath of the center of the region.

This allows us to obtain a global trend of the variations of the parameters along the swath. Parameters that are too far from this global trend are likely to be degenerate cases and the parameters are set to the value of the curve at this position. Parameters that are close enough to the value of the curve are kept, allowing for local variations in the class parameters.

2.3 Optimization

Classical methods used for Markov Random Field optimization such as ICM (iterated conditional modes) and simulated annealing can be used to solve this problem. As we are in the framework of a binary classification task, we can use the optimization introduced in [8]. This method allows us to find the global optimum by constructing a graph on which a s-t cut corresponds to a solution of our problem. The global optimum is found using a min-cut algorithm [3] corresponding to the solution having the minimum energy. To perform the optimization when using more than 2 classes, one could use α-β swap or α-expansion [2].

3 Results

Dataset To illustrate the results of this method we compute the results obtained in the framework of water detection on two images:

1. Kaw, French Guiana, acquired by TropiSAR in **Figure 3**.

2. Camargue, France, SWOT simulation (2-Looks) ([4]) in **Figure 4**.

Quantitative criteria For each classification output show the error rate, which is defined as:

$$\frac{FP + FN}{TP + FN}, \qquad (6)$$

where FP is the number of pixels incorrectly classified as water, FN is the number of pixels incorrectly classified as background and TP is the number of pixels correctly classified as water.

For each of these images, we provide the results obtained:

- Using the initial classification;

- Using the classical Markov Random Fields (one parameter for each class) with the same number of iterations that were run for the image with the Non-Uniform Markov Random Fields.

- Using the proposed method.

Discussion We can see that using our method greatly improves the results for TropiSAR data compared to the classical Markov Random Fields, but provides a limited improvement for SWOT images.

This can be explained by the contrast between the extremities of the images and the center of the antenna pattern. This contrast is of 1.56 for the SWOT image, and of 4.79 for the TropiSAR image. With a high contrast between same class parameters across the image, the classical Markov Random Fields will achieve poor results while the proposed method is able to give better estimates.

(a) Input image **(b)** Initial classification, error rate = 48.45% **(c)** Uniform MRF, error rate = 5.81% **(d)** Non Uniform MRF, error rate = 5.63%
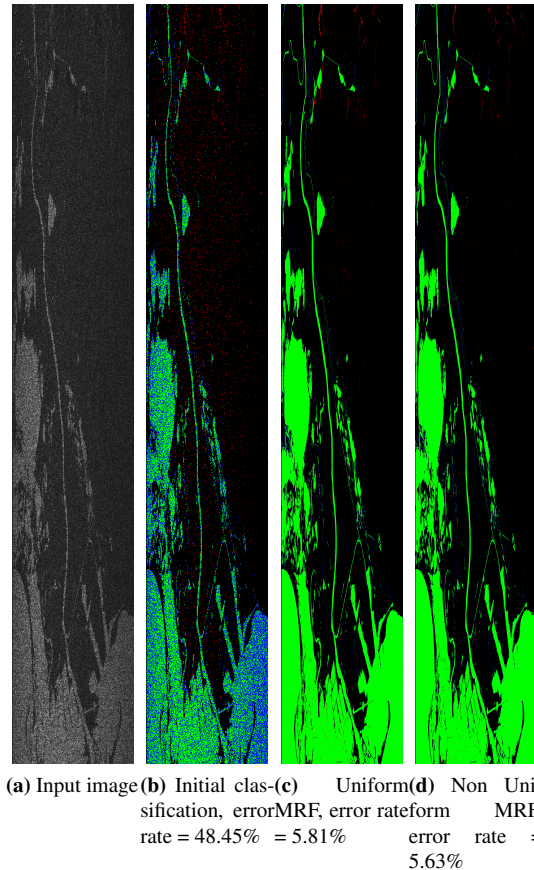
Figure 4: Results on Camargue area, Simulated SWOT images. Green: true positive, red: false negative, black: true negative and blue: false positive. Input image provided by [4].

4 Conclusions

This paper introduces a classification method suited to SAR data presenting variations of the class parameters along the swath. This method can improve the results when dealing with images with an antenna pattern not fully corrected, for instance like SWOT or TropiSAR data.

Further work includes partitioning improvement not limited to rectangles.
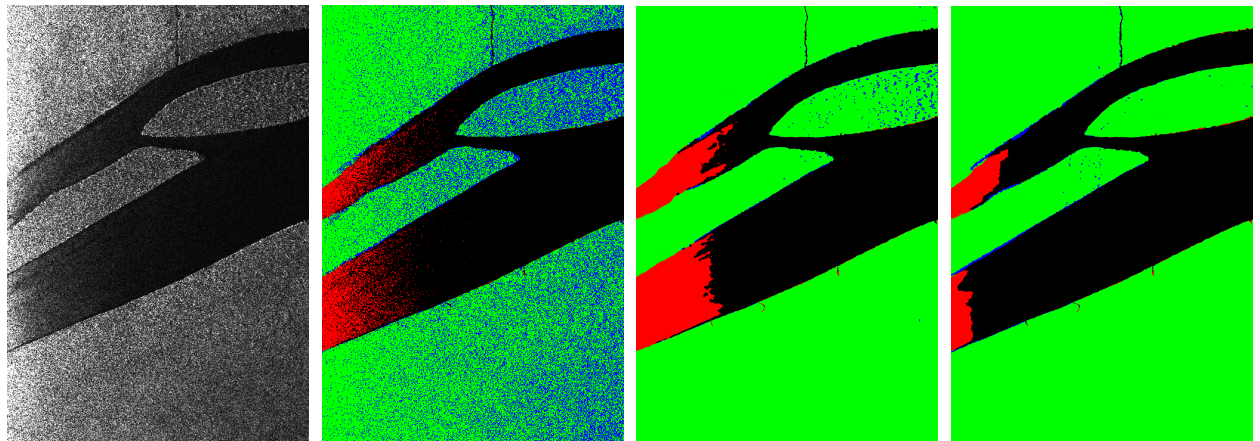
(a) Input image   **(b)** Initial classification, error rate = 34.56%   **(c)** Uniform MRF, error rate = 11.37%   **(d)** Non Uniform MRF, error rate = 4.49%

Figure 3: Results on Kaw area acquired with TropiSAR. Green: true positive, red: false negative, black: true negative and blue: false positive. Input image provided by ESA.

References

[1] Charles Bouman, Michael Shapiro, et al. A multi-scale random field model for bayesian image segmentation. *Image Processing, IEEE Transactions on*, 3(2):162–177, 1994.

[2] Y. Boykov, O. Veksler, and R. Zabih. Fast approximate energy minimization via graph cuts. *Pattern Analysis and Machine Intelligence, IEEE Transactions on*, 23(11):1222–1239, Nov 2001.

[3] Yuri Boykov and Vladimir Kolmogorov. An experimental comparison of min-cut/max-flow algorithms for energy minimization in vision. *Pattern Analysis and Machine Intelligence, IEEE Transactions on*, 26(9):1124–1137, 2004.

[4] Damien Desroches, Jean-Marc Gaudin, Roger Fjortoft, Didier Massonnet, Javier Duro, and Nadine Pourthie. Water height restitution without control points proposed for SWOT high rate mode. *Submitted to Geoscience and Remote Sensing, IEEE Transactions on*, 2015.

[5] R. Fjortoft, J.-M. Gaudin, N. Pourthie, J.-C. Lalaurie, A. Mallet, J.-F. Nouvel, J. Martinot-Lagarde, H. Oriot, P. Borderies, C. Ruiz, and S. Daniel. KaRIn on SWOT: Characteristics of Near-Nadir Ka-Band Interferometric SAR Imagery. *Geoscience and Remote Sensing, IEEE Transactions on*, 52(4):2172–2185, April 2014.

[6] Stuart Geman and D. Geman. Stochastic relaxation, gibbs distributions, and the bayesian restoration of images. *Pattern Analysis and Machine Intelligence, IEEE Transactions on*, PAMI-6(6):721–741, Nov 1984.

[7] Joseph W Goodman. *Speckle phenomena in optics: theory and applications*. Roberts and Company Publishers, 2007.

[8] DM Greig, BT Porteous, and Allan H Seheult. Exact maximum a posteriori estimation for binary images. *Journal of the Royal Statistical Society. Series B (Methodological)*, pages 271–279, 1989.

[9] Hanan Samet. The quadtree and related hierarchical data structures. *ACM Comput. Surv.*, 16(2):187–260, jun 1984.

[10] Gary J Sullivan and Richard L Baker. Efficient quadtree coding of images and video. *Image Processing, IEEE Transactions on*, 3(3):327–331, 1994.